Development of a Multi-Phase Mission Planning Tool for NASA X-57 Maxwell

Sydney L. Schnulo,* Jeffrey C. Chin,† Robert D. Falck‡ and Justin S. Gray§
NASA Glenn Research Center, Cleveland, OH, 44135

Kurt V. Papathakis, ¶ Sean Clarke, ‖ and Nickelle Reid **
NASA Armstrong Flight Research Center, Edwards, CA, 93523

Nicholas K. Borer††
NASA Langley Research Center, Hampton, VA, 23681

The physical design and operation of electric aircraft like NASA Maxwell X-57 are significantly different than conventionally fueled aircraft. Operational optimization will require close coupling of aerodynamics, propulsion, and power. To address the uncertainty of electric aircraft operation, a system level Mission Planning Tool is developed to simulate all aircraft trajectory phases: taxi, motor run-up, takeoff, climb, cruise, and descent. The Mission Planning Tool captures performance parameters at each point of the trajectory including battery state of charge, the temperatures of components in the electrical system, and propulsion system thrust. This work describes the modeling of each mission phase, and compares the results of simulating a user-specified trajectory, and using a collocated optimal control approach to determine an optimal trajectory. The results show that optimization of the mission show a significant increase in the final battery state of charge over the user-specified simulation strategy. These results will inform the operation of the NASA Maxwell X-57 test flights that will take place this year.

Nomenclature

A	Area
α	Angle of Attack
γ	Flight Path Angle
c_f	Flow Coefficient
c_p	Specific Heat
C_L	Coefficient of Lift
C_D	Coefficient of Drag
D	Drag
η	Efficiency
F_T	Thrust
h	Altitude
$\dot{h}$	Climb Rate
h_{conv}	Convective Heat Transfer Coefficient
I	Current
L	Lift
λ	Flow Coefficient Scale Factor
m	Aircraft Mass
μ_r	Rolling Resistance Coefficient
n	Load Factor
P	Power
$\dot{Q}$	Heat Rate
q	Dynamic Pressure
r	Range
R	Resistivity

*Aerospace Engineer, Propulsion Systems Analysis Branch, sydney.l.schnulo@nasa.gov, and AIAA Member.
†Aerospace Engineer, Propulsion Systems Analysis Branch, jeffrey.c.chin@nasa.gov, and AIAA Member.
‡Aerospace Engineer, Mission Architecture and Analysis Branch, rfalck@nasa.gov, and AIAA Member.
§Aerospace Engineer, Propulsion Systems Analysis Branch, justin.s.gray@nasa.gov, and AIAA Member.
¶Aerospace Engineer, Vehicle Integration and Test Branch, kurt.v.papathakis@nasa.gov, and AIAA Member.
‖SCEPTOR Principle Investigator, Systems Development Branch, Sean.Clarke@nasa.gov, AIAA Member.
**Pathways Student, Vehicle Integration and Test Branch, Nickelle.Reid@nasa.gov, AIAA Member
††Technical Lead/Aerospace Engineer, Aeronautics Systems Analysis Branch, MS 442, AIAA Senior Member.

ρ Air Density
rpm Revolutions per minute
S Wing Reference Area
SOC State of Charge
T Temperature
TAS True Airspeed
U_{Th} Thevenin Equivalent Circuit Voltage
v Ground Roll Velocity
W Aircraft Weight

I. Introduction

The Mission Planning Tool (MPT) simulates the trajectory of a fully electric aircraft through taxi, motor run-up, takeoff, climb, cruise, and descent. This multidisciplinary tool predicts the performance of the aerodynamics, propulsion, and electric systems to the fidelity necessary to predict aircraft level performance parameters such as state of charge, flight trajectory, lift, drag, motor power, and electric component temperatures. The tool is developed for NASA's experimental fully electric aircraft, Maxwell X-57 (Figure 1).

Figure 1: NASA's Scalable Convergent Electric Propulsion Technology Operations Research (SCEPTOR) final Mod IV fully electric X-57 aircraft concept with distributed propulsion.

The X-57 Modification II aircraft is available as a use case for a tool that can be used to either simulate a specified trajectory or optimize a trajectory to an objective function. The optimized trajectory is achieved through a Legendre-Gauss-Radau collocation optimal control approach. The results have shown that through optimization, we can identify a trajectory that uses 34 percent less energy than a user-specified simulation approach while assuring power and thermal constraints are satisfied. The user specified trajectory comes from the original planning of the X-57 mission for power and performance requirements. The optimized trajectory is used to inform the operation of X-57 through its test flights to achieve NASA program goals.

A. Background and Motivation

NASA's Maxwell X-57 was developed through the Scalable Convergent Electric Propulsion Technology and Operations Research subproject. It is a testbed that aims to demonstrate 4.8 times less energy consumption at cruise than a baseline piston engine powered Tecnam P2006T.[1] This reduction in energy consumption is enabled by distributed electric propulsion.[2] As seen in Figure 1, the X-57 has two large electric motor driven cruise propellers at the wingtips and six high lift electric propulsors that span each high aspect ratio wing. The high aspect ratio wing has three times less area then the baseline Tecnam airfoil, which reduces drag significantly. The six high lift propulsors on each wing augment lift of the high aspect ratio wing at takeoff and landing. At cruise, the high lift propeller blades fold back into the nacelle pods to minimize drag, while the larger wingtip cruise motors provide all of the propulsion.

The Maxwell X-57 is being developed in a series of four progressively complex modifications, referred to as mods. Mod IV is the concept previously described and shown in Figure 1. Mod I is the Tecnam P2006T. Mod II is the Tecnam P2006T converted to a fully electric aircraft. Mod II is the focus of the Mission

Planning Tool as presented in this work, and is shown in Figure 2.

Figure 2: NASA's Scalable Convergent Electric Propulsion Technology Operations Research (SCEPTOR) final Mod II fully electric X-57 aircraft concept.

The two Rotax engines are replaced with 60 kW motors, and the batteries reside in the fuselage. The Tecnam wings, propellers, and fuselage remain. The results shown in this work are from a Mission Planning Tool for the Mod II aircraft, the subject of flight tests in the coming year.

Many test flights of the Mod II aircraft will occur to assess its performance at different operating conditions. Predicting the battery state of charge throughout these planned missions is essential to maximize the number of flights and test data. It is also important to ensure that the component temperatures are not exceeding their limits, causing damage to the aircraft, and creating unsafe flight conditions. For these reasons, a Mission Planning Tool is developed to inform the test flights of the Maxwell X-57. The tool predicts battery state of charge and component temperatures either throughout a prescribed mission or a mission that is optimized for maximum battery state of charge at the end of the mission. The mission shown in Table 1 is the explicitly prescribed mission that is used in this work. It is the baseline mission being used by the SCEPTOR team for component performance requirements.

Table 1: Nominal X-57 mission.

Segment	**Velocity** kn	**time** s
Taxi	24.0	600
Motor Run-up	0.0	30
Takeoff	0.0 to 64.0	10
Initial climb to 1500 ft	64.0 to 105.0	120
Climb to 8000 ft	105.0 to 135.0	540
Cruise	135.	300
Descend to 1500 ft	135.0 to 105.0	450
Final Approach	105.0 to 64.0	180

As the first few test flights occur, any discrepancies between the flight data and the MPT predicted performance will be reconciled. The flight data will inform necessary adjustments to the assumptions made within the tool, such as heat transfer coefficients, efficiencies, aerodynamic performance parameters, and transmission losses. The flexibility of the tool to these assumptions will result in a Mission Planning Tool that predicts performance of the NASA Maxwell X-57 while minimizing error, ensuring safer and more effective operations.

B. Previous Work

The mission planning tool builds off of two significant previous efforts. From Falck's 2017 work, we derive the methods used for the modeling of the aircraft as well as the optimization schemes.[3] Original inspiration for this work comes from version 1 of the Mission Planning Tool, which acted as a first cut at system level analyses of X-57 and provided insights via trade studies.

1. Trajectory Optimization of Electric Aircraft Subject to Subsystem Thermal Constraints

The mission profile tool, developed for the SCEPTOR Maxwell Mod II aircraft, builds on the previous work by Falck.[3] Falck modeled climb from 1000 m and cruise, but does not consider any other phases of flight. The work was notionally modeled modeled for the SCEPTOR Mod III aircraft, which adds the high aspect ratio wing and wingtip propulsors. Falck's work demonstrated the dependence of the aircraft performance on the thermal constraints of the motor. The temperature limit of the motor is 100°C. The trajectory showed that that when the aircraft approaches the thermal constraint, it adjusted its climb rate, using less power to stay within temperature limits. This demonstrated the ability to optimize electric aircraft cruise trajectory with respect to thermal constraints. By using a slightly different approach, the optimizer was used to maximize state of charge at the end of the mission in order to yield the trajectory with the lowest energy consumption. The MPT builds on this work by using the same optimal control methods, but extending them to all phases of flight and customizing the model to the X-57 Mod II aircraft. The Mission Planning Tool will use end of mission state of charge as the optimization objective.

2. Mission Planning Tool Version I

The Mission Planning Tool presented in this work was motivated by one in which trade studies were done to assess mission sensitivity to climb rate, cruise time, cruise height, and cruise speed. Figure 3 shows a sample output of this tool. By determining the power required to satisfy the equations of motion for each phase, the battery energy consumption was calculated. For taxi, thrust must be equal to the friction force preventing motion, and power required was calculated as thrust multiplied by velocity.

There is an assumed power draw at takeoff. Equation 1 determined the power required at climb.

$$P_{req} = -\dot{h} * W + P_{max} \tag{1}$$

In MPT Version 1, it was assumed that the aircraft glides in descent, therefore no power is used. It also modeled the aircraft banking maneuver. The current Mission Planning Tool assumes a powered descent and a 2-dimensional trajectory, although these options will be explored in later versions. Figure 3 shows the results of a sensitivity study of the mission energy versus the cruise altitude.

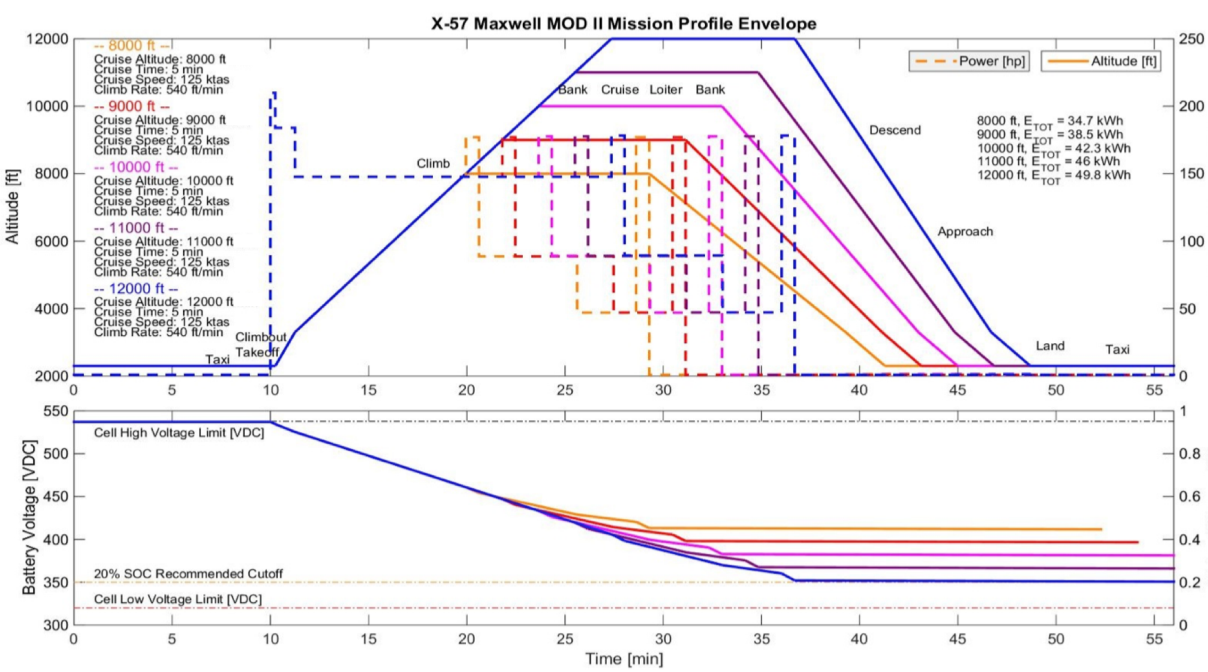

Figure 3: Cruise altitude trade study results from version 1 of the Mission Planning Tool.

The results showed that every 1000 feet of altitude costs about 6 percent state of charge. The sensitivities discovered here motivated a more complete model of the Maxwell X-57 Mod II Aircraft which also tracks electric component temperatures. The MPT presented in this paper builds on this approach by using coupled aerodynamics and electric system to predict power required, capturing electric component temperatures, and integrating a battery model that captures the discharge effects on the battery as a function of state of charge and temperature.

II. Approach

The modeling for the Mission Planning Tool is implemented using OpenMDAO, NASA's modular MDAO framework with support for efficient gradient based optimization using analytic derivatives.[4,5] We explore two different approaches for explicit and an implicit method of modeling a trajectory for the mission planning of the X-57. In the explicit mode, the user specifies an altitude, time, and speed profile that the aircraft physics are integrated through. The implicit method uses a pseudospectral optimal control method[6,7] built in the OpenMDAO framework to find the optimal trajectory. For both methods, there are controls and states. Controls are specified through the trajectory either by the user in the explicit case or the optimizer in the implicit case. States are parameters that we calculate rates for in the model in order to track their time history throughout the mission. In explicit mode, the states are integrated using the Scipy integrate function.[8] In implicit mode, state time histories are solved for using an Legendre-Gauss-Radau (LGR) pseudospectral collocation scheme.[9,10] These overarching methods are wrapped around the subsystems that model the physics of the aircraft, which are described in the subsequent section.

III. Subsystem Modeling

The aerodynamics group calculates vehicle level aerodynamic coefficients (C_L and C_D), lift, drag, and angle of attack based on flight conditions, as shown in Figure 4.

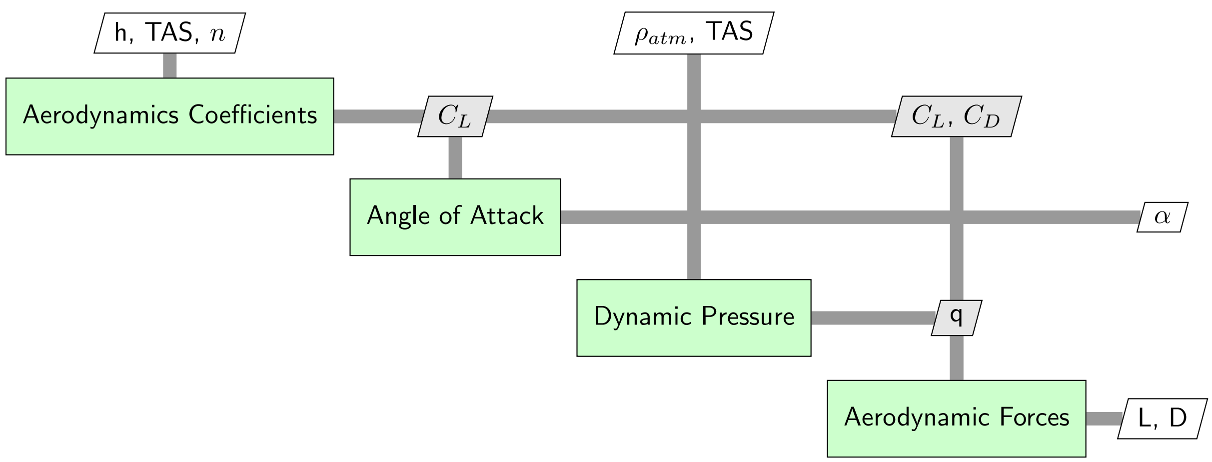

Figure 4: Aerodynamic group model with inputs and outputs.

C_L and C_D are interpolated as a function of altitude, true airspeed, and load factor (L/W). This table was assembled using flight data from the baseline Tecnam P2006T aircraft. The angle of attack is calculated using equation 2

$$\alpha = (C_L - C_{L0})/C_{La} \tag{2}$$

where C_{La} and C_{L0} are derived from Tecnam P2006T aircraft data.[11] Lift and drag are found using dynamic pressure, wing reference area, C_L, and C_D, shown in equations 3 and 4.

$$L = q * S * C_L \tag{3}$$

$$D = q * S * C_D \tag{4}$$

Angle of attack, lift, and drag are critical when calculating the flight dynamics of the aircraft, which will be described in a later section. This group models the aerodynamics of the mod II aircraft. In mod IV, it will be necessary to add models of the high lift motors and include their impact on aircraft lift and drag.

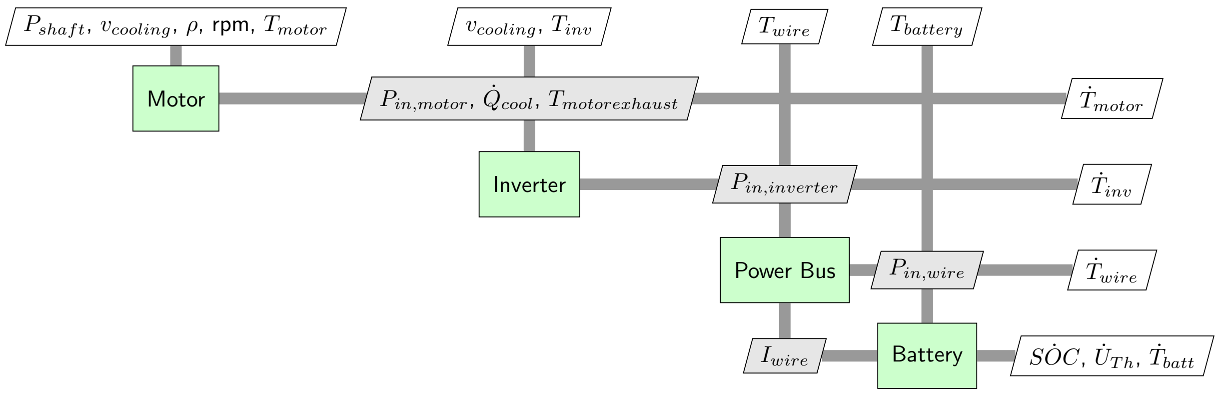

Figure 5: Electric system model that includes battery, power bus, inverter, and motor components.

The electric group includes components that model the motor, the inverter, the power bus, and the battery, as shown in Figure 5. On the aircraft, power flows from the battery, through the power bus, to the inverter, to the motor which provides shaft power to the propeller. However, to accommodate the overall aircraft modeling approach, the electric group accepts an input of shaft power required at the motor. We can then calculate the power required through each of the electrical components, factoring in the respective losses, to determine the load that the battery must provide. Along with power, transient thermal load calculations are implemented in the electric group with bulk thermal parameters estimated by previous work by Chin.[12] The out-runner permanent magnet motor is cooled by the propeller exhaust air that flows through an annular heat sink.[13,14] This air then cools the inverter in series. This requires another input to the electric group: velocity of the air aft of the propeller that the inverter heat exchanger sees ($v_{cooling}$). The motor component yields the efficiency and thermal behavior of the two Joby Aviation 60 kW motors that are on the mod II aircraft. The efficiency is found by interpolating proprietary data that comes from the motor manufacturers as a function of shaft speed and torque. Shaft speed is a control, therefore torque is defined as the input shaft power divided by shaft speed. With shaft speed and torque, the efficiency is interpolated from the performance table. The efficiency then dictates the power that must be supplied from the inverter. Efficiency also factors into the heat load that the motor sees, as seen in equation 5.

$$\dot{Q}_{motor} = P_{motor}(1 - \eta_{motor}) \tag{5}$$

The heat that the motor heat sink dissipates is estimated by assuming a convective heat transfer coefficient and using equation 6.

$$\dot{Q}_{cool} = h_{conv}A(T_{motor} - T_{\infty}) \tag{6}$$

The rate of change in motor temperature is the difference between the heat load of the motor and the cooling rate ($\dot{Q}_{motor} - \dot{Q}_{cool}$), divided by the heat capacity of the motor. Because the motor and the inverter are cooled in series, the temperature of the air after it cools the motor is necessary to predict the inverter temperature. The temperature rise of the motor heat sink exhaust is computed in equation 7. The exhaust temperature is computed by multiplying the inlet dynamic pressure by a laminar flow coefficient with an additional scaling factor (λ) to compensate for extrapolating an individual flow model to fit the entire heat sink.

$$T_{motorexhaust} = T_{\infty} + \frac{\lambda * \dot{Q}_{cool}}{\rho^2 * v_{cooling}^2 * c_f * c_p} \tag{7}$$

The inverter is modeled in a similar way. We assume an efficiency to determine the power that must be supplied by the battery. That loss determines the heat generated in the inverter, and the cooling flux is calculated the same way, but with motor exhaust temperature as the ambient temperature. The power bus losses are calculated by using the resistivity of copper wire and assuming Joule heating (I^2R), requiring current to be input from the battery model.

The battery is modeled at the cell level as a Thevenin equivalent circuit,[15] which is then multiplied to supply pack level power, current, and battery state rates, as was done in Falck's aircraft model.[3] This modeling method captures the transient response of the battery with respect to temperature and state of charge. The performance maps come from arbitrary lithium ion battery data.[15] It supplies the rates of battery temperature and Thevenin voltage. The model also solves for the system current given the power required by the power bus component for its Joule heating calculation.

The propeller model is also based off of Falck's model. Its inputs are true airspeed, air density, and rpm. Depending on the context of the aircraft model, it also takes an input of shaft power and calculates thrust, or vice versa. The model either calculates thrust analytically, or uses a Newton solver to solve for the power required to achieve the input thrust. The model also calculates the velocity of the air aft of the propeller to inform the motor cooling model. Because the electric group only models one half of the aircraft, the thrust of one propeller is multiplied by two in this group to give the overall thrust of the aircraft.

IV. Phases of Flight and Dynamics

The Mission Profile Tool has the ability to model all segments of Maxwell X-57's flight. These include taxi, motor run-up, takeoff, climb, cruise, and descent. It assumes a two-dimensional flight path. Each phase of flight requires different dynamics, states, and controls to model them to the fidelity needed for mission planning. All phases track state of charge, battery temperature, power bus temperature, inverter temperature, and motor temperature as states. In the component models, the rate of change of these components is computed analytically to allow the model to capture the behavior over the trajectory.

A. Taxi

In taxi, we assume that ground speed is constant over a specified amount of time. Because of this assumption, the acceleration term becomes zero in equation 8,

$$0 = F_T - D - \mu_r(W - L) \tag{8}$$

where F_T is thrust, D is drag, μ_r is the rolling friction coefficient, W is aircraft weight, and L is lift. This equation yields the thrust required to achieve this taxi speed, and this required thrust is input into the propeller model, as seen in Figure 6. A Newton solver determines the thrust that achieves constant speed.

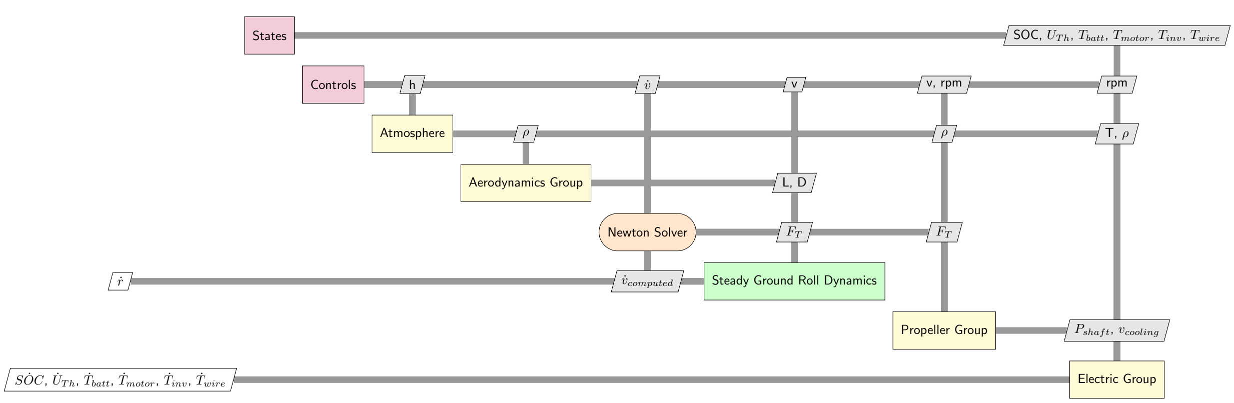

Figure 6: Taxi phase model of a constant speed ground roll.

The propeller model then solves for the shaft power required to provide the input thrust value. The electric group uses the shaft power value as an input value to solve through the system and estimate the battery energy usage state, as well as component temperature states. Range is an additional state that applies to taxi, and the rate is simply the speed of the aircraft, which is a control specified by the user or the optimizer.

B. Motor Run Up

The motor run up consists of a user defined throttle setting of the motors and running the motors at that power level. It is a relatively simple phase, as it does not require any aircraft dynamics. The state of charge of the batteries and component temperatures are the only state variables that need to be tracked. The groups used in this phase are the electric group, the propeller group, and the throttle group, as seen in Figure 7.

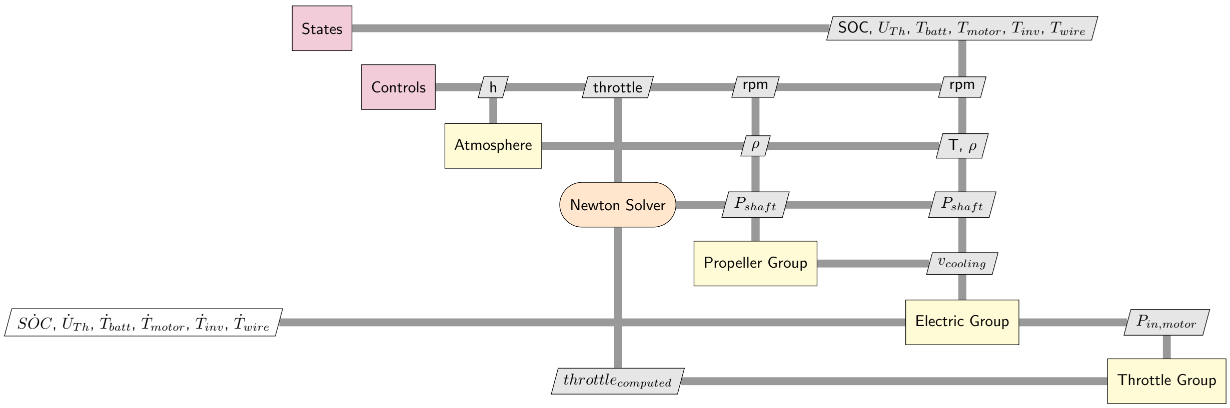

Figure 7: Motor run up phase architecture which runs the electric system at a certain throttle setting.

The user inputs the throttle at which the motor should be run. This value is between 0 and 1 as percentage of maximum continuous power. The throttle group calculates the commanded input power of the motor. The group level Newton solver varies the shaft power until the power into the motor that is calculated by the electrics group matches this input motor power. The implicitly determined shaft power is input into the propeller group. The purpose of the propeller group in this phase is to calculate the velocity of the air aft of the propeller, which is used for motor and inverter temperature calculations.

C. Takeoff

The takeoff phase involves the aerodynamics, propeller, electric, and throttle groups, as seen in Figure 8.

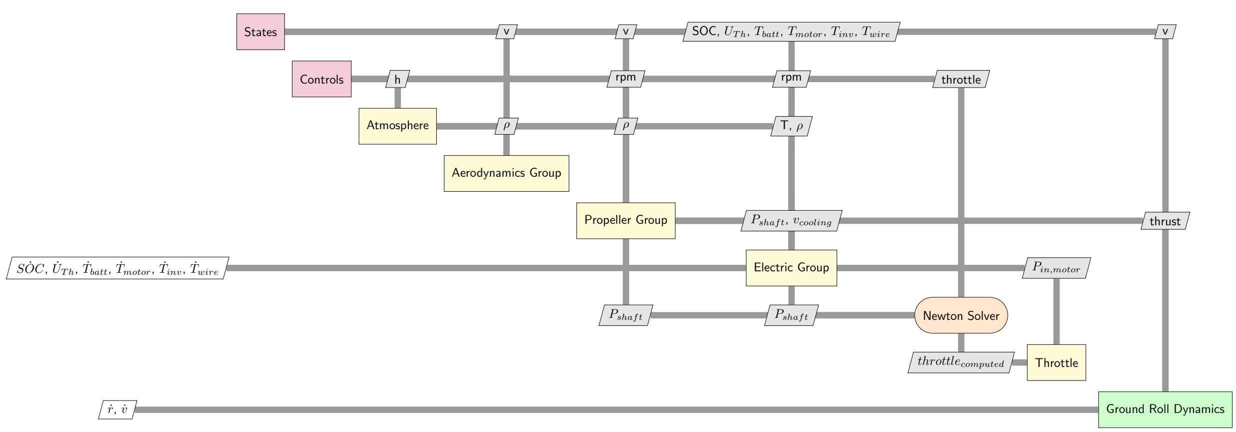

Figure 8: Takeoff phase model which captures the acceleration from zero velocity to rotational velocity.

The takeoff phase assumes that the motors are at their maximum continuous power, therefore throttle is equal to 1. It uses the throttle group in the same way that motor run up does: to find the shaft power that is supplied to the propeller after some losses through the motor. The propeller then is able to calculate thrust. The thrust value is used in equation 9, the ground roll dynamics, to find acceleration.

$$m\dot{v} = F_T - D - \mu_r(W - L) \tag{9}$$

In this phase, speed is a state. The acceleration computed in the ground roll dynamics supplies the rate of change, as shown in Figure 8. In explicit mode, the user specifies the the amount of time for the phase. In implicit mode, we add a nonlinear constraint that causes the optimizer to end the phase when speed reached the takeoff rotation velocity of the aircraft.

D. Climb/Cruise/Descent

The user can specify either an altitude or power profile when modeling climb, cruise, and descent. Each mode includes the aerodynamics group, the electric group, and the propeller group, but with different states and controls. The flight dynamics remain the same for each mission. The physics are derived from the free body diagram in Figure 9.

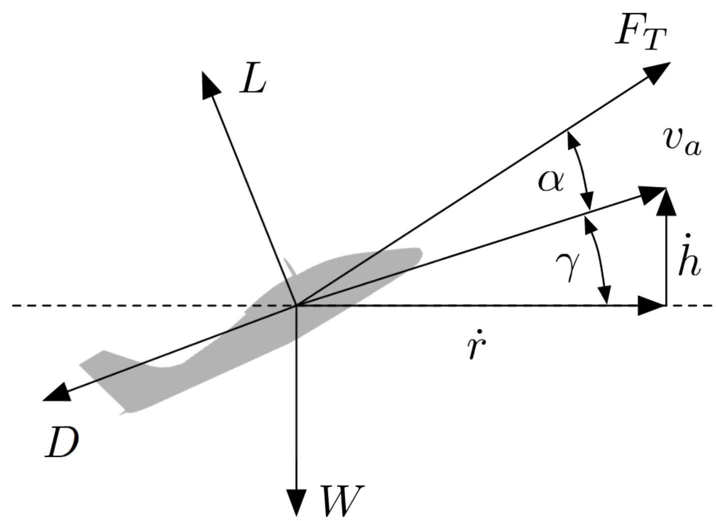

Figure 9: Free body diagram of aircraft dynamics.

The unsteady flight dynamics yield the acceleration and the rate of change in flight path angle, shown in equations 10 and 11.

$$T\dot{A}S = \frac{F_T * cos\alpha - D}{m} - g * sin\gamma \tag{10}$$

$$\dot{\gamma} = \frac{F_T * sin\alpha + L}{mTAS} - \frac{g * cos\gamma}{TAS} \tag{11}$$

Climb, cruise, and descent can be modeled in two modes. In the first, altitude and true airspeed are controls. This means that either the user specifies the values of the controls in explicit mode or the optimizer chooses the values in the implicit mode. Figure 10 shows the model architecture of the prescribed altitude flight phase. The states in this phase are range, state of charge of the battery, Thevenin voltage, and component temperatures. The controls are altitude, therefore altitude's rate and second derivative, true airspeed, acceleration, and shaft speed. We find flight path angle and its rate using equations 12 and equation 13, respectively.

$$\gamma = sin^{-1}(\frac{\dot{h}}{TAS}) \tag{12}$$

$$\dot{\gamma} = \frac{TAS * \ddot{h} - \dot{h} * T\dot{A}S}{TAS^2 * \sqrt{1 - (\frac{\dot{h}}{TAS})^2}} \tag{13}$$

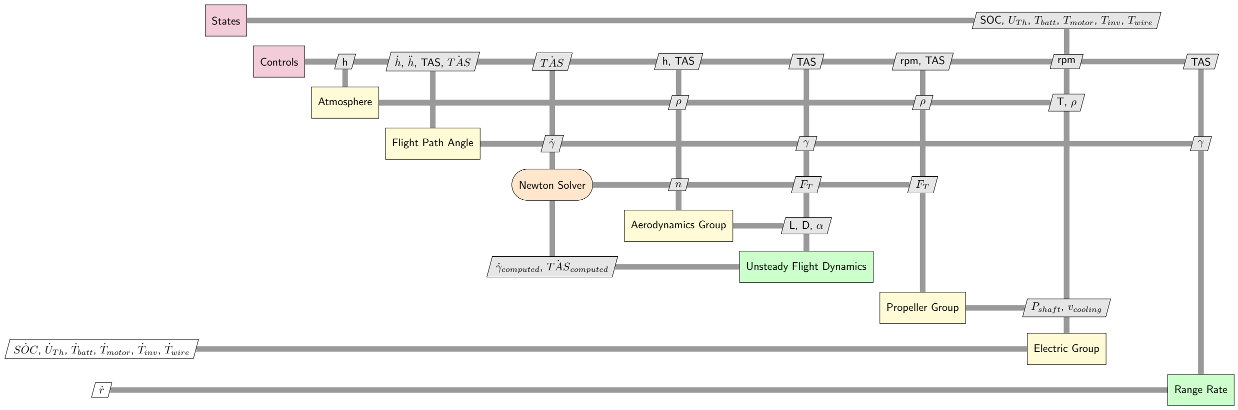

Figure 10: Altitude prescribed trajectory model that is used for climb, cruise, or descent.

We then have a Newton solver that iterates on thrust required and load factor until rate of flight path angle ($\dot{\gamma}$) computed in equations 11 and 13 agree, and acceleration from equation 10 matches acceleration from the control value. This ensures that the equations of motion are satisfied and we can determine the amount of power required from the electric system. Range rate is calculated in equation 14.

$$\dot{r} = TAS * cos\gamma \tag{14}$$

It is also beneficial to have a phase option in which power is a control. This is favorable in operation; the pilot often flies at a constant throttle setting. Another phase was developed to accommodate this reality in mission planning. The power prescribed model is shown in Figure 11.

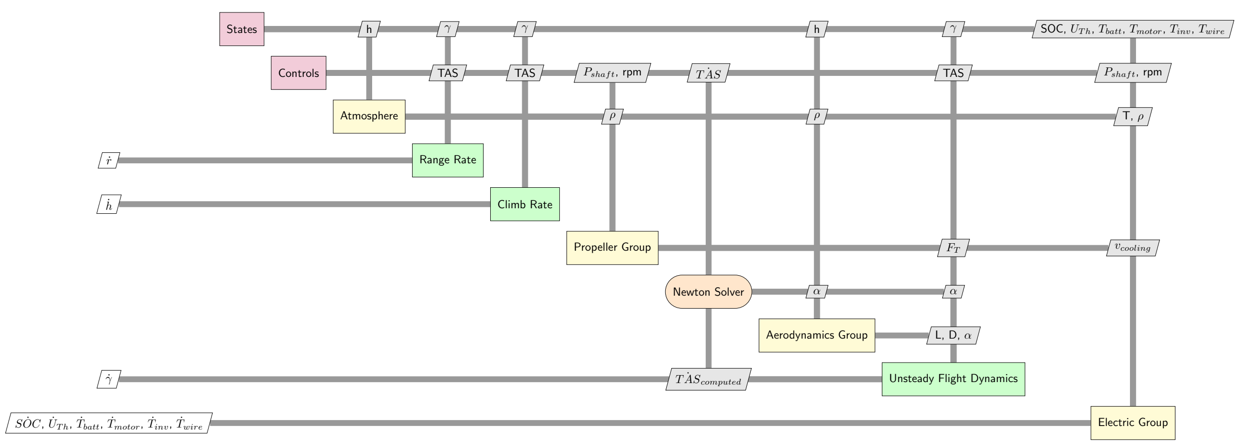

Figure 11: Power controlled model that can be used for climb, cruise, or descent.

Here, we make shaft power a control rather than altitude. To satisfy our equations of motion, we make flight path angle a state. True airspeed and rpm remain controls. Range rate is found using true airspeed and flight path angle as was done in equation 14, and climb rate is calculated using equation 15.

$$\dot{h} = TAS * sin\gamma \tag{15}$$

Shaft power is input to the propeller, which provides the thrust to the unsteady flight dynamics. A Newton solver finds the value of angle of attack to satisfy the flight dynamics such that acceleration computed is equal to acceleration dictated by the control. This method allows the modeling of a constant power trajectory.

V. Results and Discussion

The phases of flight are linked together in both an explicit and an implicit solution. In the explicit solution, the aircraft is given a prescribed altitude and true airspeed profile. The states are then integrated throughout the mission. In the implicit solution, the optimizer chooses the control values in order to maximize battery state of charge at the end of the mission. The optimized solution yields 28 percent higher state of charge, and therefore less energy consumption, at the end of the mission.

A. Explicit Solution

In the explicit solution, we show a simulation strategy in which a trajectory's speed, altitude, and time at each phase is input by the user. The initial and final conditions of each phase are specified and linearly interpolated through the phase. The MPT then uses a Scipy integrator to update the states and simulate the trajectory. The simulated mission is the reference mission from Table 1. As an implementation example, in the initial climb phase we specify that the initial velocity is 64 kn, and the velocity at the end of the phase after climbing 1500 ft is 105 kn. We use the altitude controlled climb model described. The controls true airspeed and altitude are linearly interpolated from 64 kn to 105 kn, and ground level to 1500 ft above ground level, respectively. This approach is also taken for climb, descent, and final approach. The simulation results are shown in Figure 12, where altitude is specified as above mean sea level at NASA Armstrong Flight Research Center in Edwards, California.

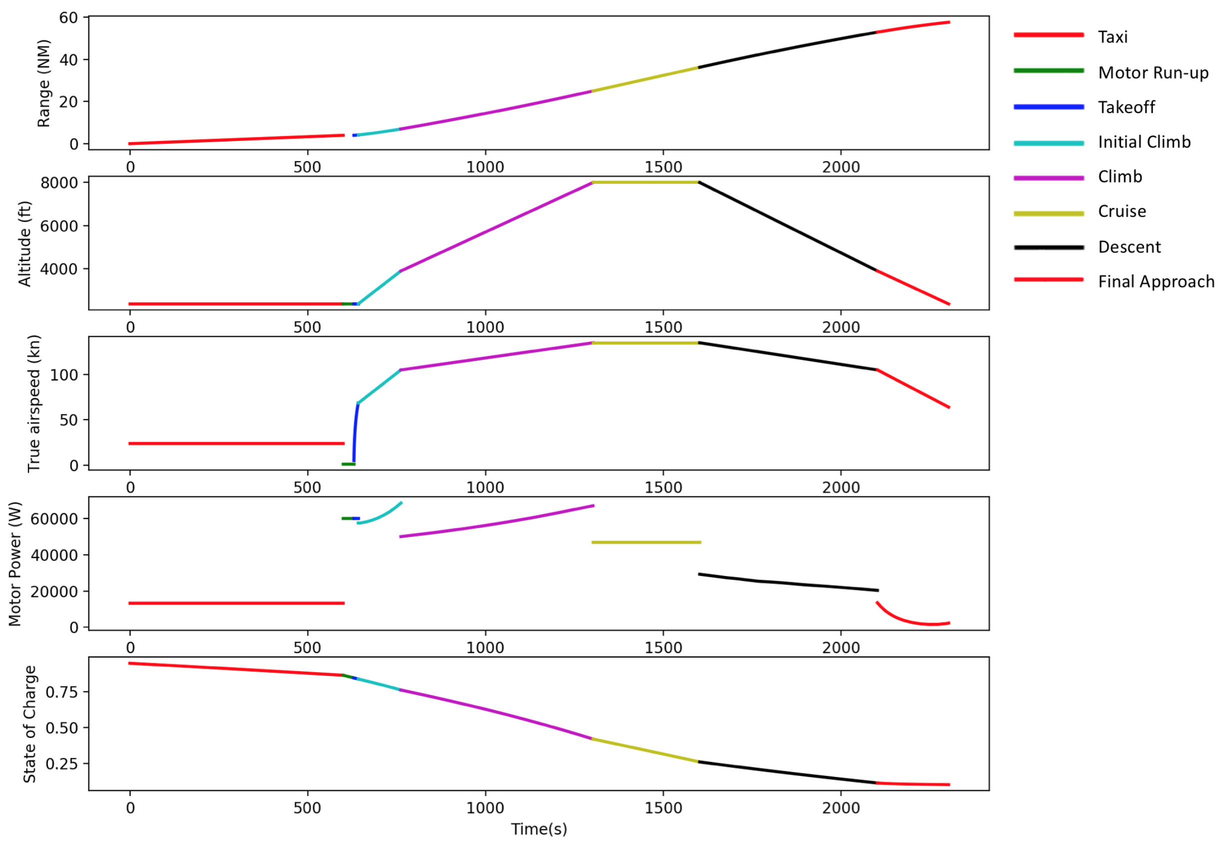

Figure 12: Mission trajectory results of the explicit solution.

The explicit simulation results in an end of mission state of charge of 10 percent, draining 85 percent from the 95 percent initial state of charge and using 44.1 kWh. The trajectory has a range of 57 nautical miles. The power required per motor at cruise is 46.5 kW. The power profile shows a widely varying throttle at each point of initial climb in order to achieve the linearly interpolated power and altitude profile. Requiring the pilot to vary throttle setting continuously at climb and descent is not a realistic way for the aircraft to fly. We also see that flying this trajectory requires more than 60 kW per motor at certain points of the mission. This is a problem as 60 kW is the maximum continuous power of the motors.

After determining that this mission is not practical for test flights of the X-57, there are two options. The first is to manually adjust the trajectory until we found a feasible one, while the second is to use an optimal control problem to choose a reasonable climb and descent trajectory that maximizes the end of mission state of charge. The first option is quite tedious and requires much trial and error, so we completed a trajectory optimization which can later inform prescribed trajectories.

B. Implicit Solution

In the implicit solution, the LGR pseudospectral optimal control collocation method is used. Each phase is modeled as collocated segments within an optimal control problem. Constraints are placed on the initial and final state values of each phase such that they are continuous with the phases that come before and after. In the implicit solution, the taxi, motor check, and cruise phases are prescribed to be the same as the user specified trajectory used in the explicit solution. The takeoff phase includes a boundary constraint in which the phase ends when velocity reaches the rotational velocity of the aircraft, whereas it is defined by inputting time in the explicit phase. The climb and descent phases use the power model architecture described. Constraints are placed on motor power, angle of attack, and acceleration. An upper constraint is placed on motor power such that it does not exceed 60 kW, or the maximum continuous power stated by the motor manufacturer. Angle of attack also requires an upper constraint to avoid stall. Finally, acceleration is to be positive in climb and negative in descent. The objective is set to maximize the battery state of charge at the end of the mission. The controls that the optimizer determines through the mission are takeoff time as well as the power levels and true airspeed of the aircraft through climb and descent. Figure 13 shows the optimized trajectory, where the battery state of charge is 95 percent at the start of the mission for battery health purposes.

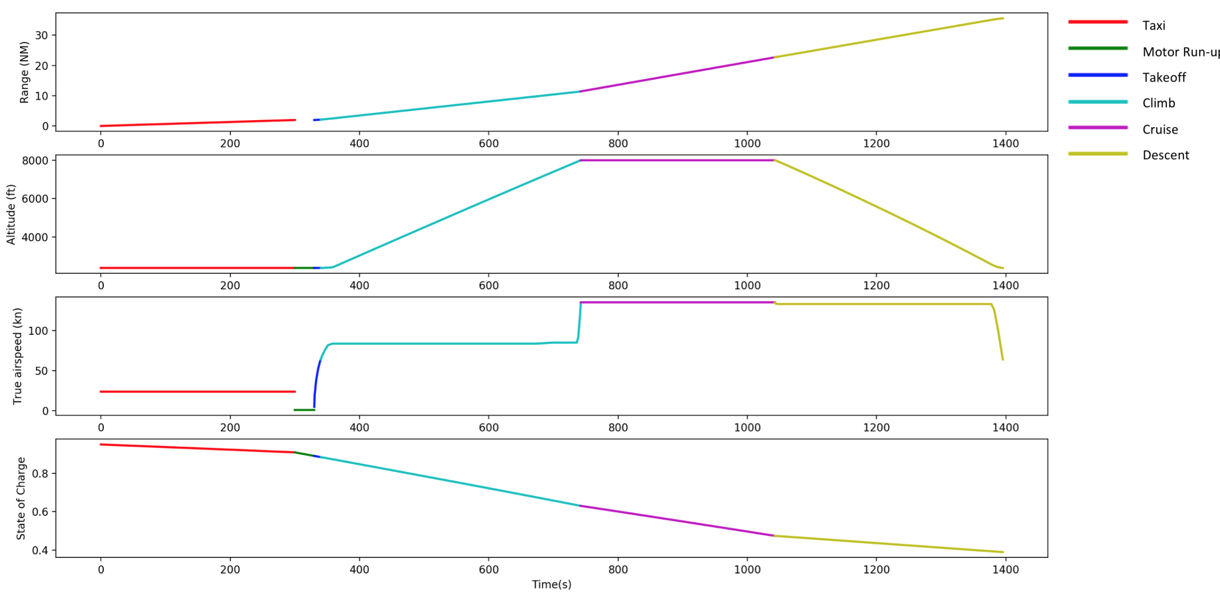

Figure 13: Results of the optimal control problem to maximize battery energy at the end of the mission.

The aircraft achieves a range of 36 nautical miles through taxi, takeoff, climb, cruise, and descent. This range is significantly lower than what the explicit simulation predicts, due to a faster climb and descent that yields lower overall range. The cruise segment, which is main portion of the flight for testing purposes, remains the same for both solutions. After 300 seconds of taxi and 30 seconds of motor check, the takeoff phase predicts that at full throttle, the aircraft will reach the rotational velocity of 64 kn in 9.9 seconds. The climb phase then predicts a climb to 8000 feet MSL in 400 s. During this climb phase, the optimizer chooses the motor power to be at its maximum of 60kW. It first accelerates at a low flight path angle to 83.5 kn before climbing at a constant true airspeed in order to maximize climb rate. Once the aircraft reaches the cruise altitude, it accelerates to the cruise speed of 135 kn. The trajectory then shows the prescribed 300 second cruise at 135 kn, before it starts to descend. For descent, the true airspeed reduces slightly to 133 kn until it quickly decelerates to 64 kn. Descent takes 353 seconds, at a near constant power of 21 kW. The motor and battery temperatures, as well as motor power profile, are shown in Figure 14.

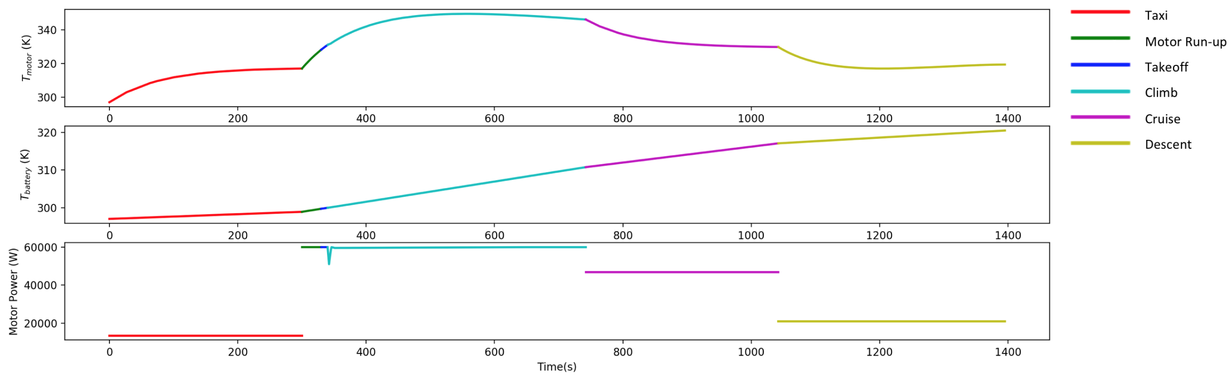

Figure 14: Component temperatures and motor powers through the implicit mission.

None of the component temperatures are exceeding their respective limits, therefore we do not add any temperature constraints to the optimization. The motor powers are fairly consistent through phases: climbing at 60 kW and descending at 21 kW. This opens up a more intuitive flight test plan for a pilot as opposed to the explicit method of simulation which shows widely varying powers through out. To follow the optimal trajectory, the pilot simply accelerates to 83.5 kn after takeoff before climbing to cruise altitude at full power. Once at cruise altitude, climb stops and the aircraft accelerates to the cruise speed. After cruise, the pilot throttles back to 21 kW for descent. This is similar to the operation of general aviation aircraft, and the optimal control problem verifies that this is the most efficient way to fly, with a final battery state of charge of 38 percent using a total of 30 kWh. The optimized trajectory used 32 percent less energy in than the manually specified trajectory modeled with the explicit simulation.

Figure 3 showed every 1000 feet of altitude cost about 6 percent state of charge at the end of the mission. That study is replicated with the current Mission Planning tool, using the implicit simulation in order to compare the results from the two cases. Using the full aircraft dynamics and a powered descent, the tool predicts an average of 5.8 percent state of charge used for each 1000 feet of cruise altitude. This shows that the lower fidelity models from version 1 resulted in a slightly conservative predictions in energy consumption, but that the trend are the same and the results are in strong agreement.

These results show that optimization is worthwhile in the X-57 mission planning. As was demonstrated by the explicit and implicit results, optimization is the preferable for the ability to model real aircraft operations as it shows a lower energy consumption as well as a intuitive power profile. Because both the explicit and implicit methods use the same physics, we will still see this advantage as the aircraft model continues to mature. In future mission planning, running an optimal trajectory is the first step in finding a sensible solution, which can then be adjusted for sensitivities in the explicit solution. Therefore, both modeling strategies add overall value to the Mission Planning Tool.

VI. Conclusion

A mission planning tool that models the aerodynamic, propulsion, and electric systems of the Maxwell X-57 has been developed. The MPT captures all phases of flight: taxi, motor runup, takeoff, climb, cruise, and descent, with dynamics appropriate to each. The MPT has the option to run in two modes: explicit and implicit. In explicit mode, the user prescribes a trajectory and the aircraft states are integrated through the mission. If the MPT is run in implicit mode, the user specifies an objective and constraints for the trajectory and the optimizer will vary the controls to achieve an optimal trajectory. The implicit solution of a notional Maxwell X-57 mission yields a more operationally friendly trajectory, as well as an increase in battery state of charge at the end of the mission over the explicit solution.

The mission planning tool will continue to mature as we are able to apply experimental data. The battery model implemented includes data from an arbitrary lithium ion battery;[15] this will be replaced by performance maps obtained through cell level isothermal discharge tests of the Samsung 18650 cells that will power the X-57. Further, through flight data we will be able to better fit the performance of the tool to the performance of the aircraft. The tool allows for trajectory flexibility too; we can explore different flight test options such as the optimal cruise height or speed. The Mission Planning Tool will continue to be developed to be higher fidelity and increasingly user friendly. Further, the tool will be exercised to determine sensitivities to the assumptions used and flight trajectories.

The mission planning tool's function is to model the Maxwell X-57 mod II aircraft through different trajectories in order to plan test flights. This work shows that there is value in using collocated optimal control in mission planning for the Maxwell X-57. The optimal control approach is able to determine true airspeed and climb rate through the climb and descent phases to identify a trajectory that uses 32 percent less energy than the explicitly simulated trajectory with near constant throttle settings. This is evidence that the use of optimization in the mission planning tool will provide more efficient and pilot friendly trajectories for the planning of the Maxwell X-57 Modification II missions.

VII. Acknowledgements

The authors would like to thank the Flight Development Capabilities and Transformational Tools and Technologies projects for their support of this work.

References

[1]Borer, N. K., Patterson, M. D., Viken, J. K., Moore, M. D., Bevirt, J., Stoll, A. M., and Gibson, A. R., "Design and Performance of the NASA SCEPTOR Distributed Electric Propulsion Flight Demonstrator," *16th AIAA Aviation Technology, Integration, and Operations Conference*, No. AIAA 2016-3920 in AIAA Aviation, American Institute of Aeronautics and Astronautics, June 2016.

[2]Papathakis, K., Kloesel, K., Lin, Y., Clarke, S., and Ginn, S., "Design and Development of a 200-kW Turbo-electric Distributed Propulsion Testbed," No. 2016-461 in Propulsion Energy, American Institute of Aeronautics and Astronautics.

[3]Falck, R., Chin, J., Schnulo, S., Burt, J., and Gray, J., "Trajectory Optimization of Electric Aircraft Subject to Subsystem Thermal Constraints," *18th AIAA Aviation Technology, Integration, and Operations Conference*, No. 2017-4002 in AIAA Aviation, American Institute of Aeronautics and Astronautics, June 2017.

[4]Gray, J., Moore, K., and Naylor, B., "Standard Platform for Benchmarking Multidisciplinary Design Analysis and Optimization Architectures," *AIAA Journal*, Vol. 51, No. 10, October 2013, pp. 2380–2394.

[5]Gray, J. S., Hearn, T. A., Moore, K. T., Hwang, J., Martins, J., and Ning, A., "Automatic Evaluation of Multidisciplinary Derivatives Using a Graph-Based Problem Formulation in OpenMDAO," *15th AIAA/ISSMO Multidisciplinary Analysis and Optimization Conference*, American Institute of Aeronautics and Astronautics, 2014/07/08 2014.

[6]Herman, A. L. and Conway, B. A., "Direct optimization using collocation based on high-order Gauss-Lobatto quadrature rules," *Journal of Guidance, Control, and Dynamics*, Vol. 19, No. 3, 1996, pp. 592–599.

[7]Falck, R., Gray, J., and Naylor, B., "Parallel aircraft trajectory optimization with analytic derivatives," *17th AIAA/ISSMO Multidisciplinary Analysis and Optimization Conference*, No. AIAA 2016-3207, 2016.

[8]Jones, E., Oliphant, T., Peterson, P., et al., "SciPy: Open source scientific tools for Python," 2001.

[9]Kameswaran, S. and Biegler, L. T., "Convergence rates for direct transcription of optimal control problems using collocation at Radau points," *Computational Optimization and Applications*, Vol. 41, No. 1, Sep 2008, pp. 81–126.

[10]Garg, D., Patterson, M., Hager, W. W., Rao, A. V., Benson, D. A., and T.Huntington, G., "A unified framework for the numerical solution of optimal control problems using pseudospectral methods," *Automatica*, Vol. 41, November 2010, pp. 1843–1851.

[11]Nicolosi, F. and De Marco, A., "Stability, Flying Qualities and Parameter Estimation of a Twin-Engine CS-23/FAR 23 Certified Light Aircraft," , No. 2010-7947, August 2010.

[12]Chin, J., Schnulo, S., and Smith, A., "Transient Thermal Analyses of Passive Systems on SCEPTOR X-57," *17th AIAA Aviation Technology, Integration, and Operations Conference*, No. 2017-3784, American Institute of Aeronautics and Astronautics, June 2017.

[13]Schnulo, S., Chin, J., and Smith, A., "Steady State Thermal Analyses of Wingtip Propulsor on SCEPTOR X-57," *17th AIAA Aviation Technology, Integration, and Operations Conference*, No. 2017-3783, American Institute of Aeronautics and Astronautics, June 2017.

[14]Christie, R., Dubois, A., and Derlaga, J., "Cooling of Electric Motors Used for Propulsion on SCEPTOR," *AIAA Aviation and Aeronautics Forum and Exposition*, No. GRC-E-DAA-TN32571, American Institute or Aeronautics and Astronautics, June 2016.

[15]Huria, T., Ceraolo, M., Gazzarri, J., and Jackey, R., "High Fidelity Electrical Model with Thermal Dependence for Characterization and Simulation of High Power Lithium Battery Cells," *Electric Vehicle Conference (IEVC)*, pp 1-8, IEEE International, March 2012.